DETACHED BOW SHOCK CAPTURING IN UNSTRUCTURED GRID DOMAIN

Diomar Cesar Lobão, dclobao@eeimvr.metal.uff.br
Universidade Federal Fluminense-UFF, Av. Dos Trabalhadores n. 420. Vila Santa Cecilha. Cep: 27255-125, Volta Redonda RJ. Brazil.

Abstract. *The The space-time conservation finite volume and solution on unstructured mesh method is applied to solve compressible fluid flow problems with detached bow shock. In this work an explicit Runge-Kutta of third order solver for the Euler equations that govern the flow of a compressible inviscid flow, with application to blunt bodies is presented. The Euler equations are discretized in space using an edge-based finite volume formulation on arbitrary polygonal unstructured mesh. The resulting system of nonlinear ordinary differential equations is solved using a third order Runge-Kutta explicit scheme. The solver is tested with a single airfoil in the transonic flow regime in order to validate it. In this work the solver is tested by solving the Euler equations for a set of different blunt bodies geometries and Mach numbers. It is showed that the scheme is able to capture shocks and other discontinuous solutions sharply and accurately. Results show the solver to be accurate and also competitive with other solvers.*

Keywords*: Edge-based finite volume CFD, detached bow shock simulation, Explicit Runge-Kutta third order.*

1. INTRODUCTION

The space-time conservation finite volume and solution on unstructured mesh method described as edge-based finite volume and used here is applied for external flow problem and has some key features that distinguish it from other approaches as described in (Barth, 1992), (Barth and Ohlberger, 2004), (Berglind, 2000), (Lyra *at al.* 2002a), (Lyra *at al.*, 2004b). These include a finite difference treatment of space and explicit third order Runge-Kutta scheme in time, and a thoughtfully designed grid data structure for enforcing conservation laws. The computational domain is discretized using a finite volume formulation in which the control volumes are arbitrary polygonal volumes. These volumes compose a grid**,** formed by connecting the vertexes of a triangular grid, as shown in fig. 1.

The rest of the paper is organized as this. Section 2 describes the numerical scheme. Section 3 describes the time integration. Section 4 presents numerical results for a benchmark test problem and other tests. Section 5 concludes the paper.

2. THE NUMERICAL SCHEME

The integral conservative form of the Euler equations for an unsteady, two-dimensional, compressible inviscid flow across a surface Ω, can be expressed as:

$$\frac{d}{dt}\int_{\Omega} Q dA + \int_{\Omega} \nabla . \vec{F} dA = 0 \tag{1}$$

Here Q is a vector of conserved flow variables, ***F=F(Q)*** is the inviscid flux tensor:

$$Q = \begin{bmatrix} \rho \\ \rho u \\ \rho v \\ e \end{bmatrix} \quad \vec{F} = \begin{bmatrix} \rho u \\ (\rho u^2 + p) \\ \rho uv \\ (e+p)u \end{bmatrix} \vec{i} + \begin{bmatrix} \rho v \\ \rho uv \\ (\rho v^2 + p) \\ (e+p)v \end{bmatrix} \vec{j} \tag{2}$$

The dimensional variables, density $\bar{\rho}$, velocity $\bar{u}, \bar{v}$ and total energy $\bar{e}$, are non-dimensionalized using freestream values:

$$\rho = \frac{\bar{\rho}}{\rho_\infty}; u = \frac{\bar{u}}{u_\infty}; v = \frac{\bar{v}}{v_\infty}; e = \frac{\bar{e}}{\overline{\rho_\infty a_\infty}^2} \tag{3}$$

Where $\sqrt{\gamma p / \rho}$ is the speed of sound. Pressure is related to the conserved variables by the equation of state for a perfect gas:

$$p = (\gamma - 1)\left[e - \frac{1}{2}\rho(u^2 + v^2) \right] \tag{4}$$

which provides closure for Eq.(1), by relating the thermodynamic variables.

2.1. Finite Volume Discretization

The computational domain consists of geometries multi-connected. The tessellation of this region into a collection of non-overlapping triangular control volumes is carried out using a mesh generator developed by (Persson and Strang, 2004). Their ideas are based upon a refined version of the classical Delaunay algorithm. The advantage of their mesh generator is that it is able to produce smooth and nearly equilateral triangular grids which are a desirable property for a simple finite volume method. Consider a representative volume ***k*** from the interior of the domain, whose n_{kj} is the outward normal at the edge formed by edge ***j,*** as shown in Fig. 1. The volume has an area Ω_k and outward normal defined as $n_{kj} = (\Delta y_{kj} - \Delta x_{kj})/|n_{kj}|$.

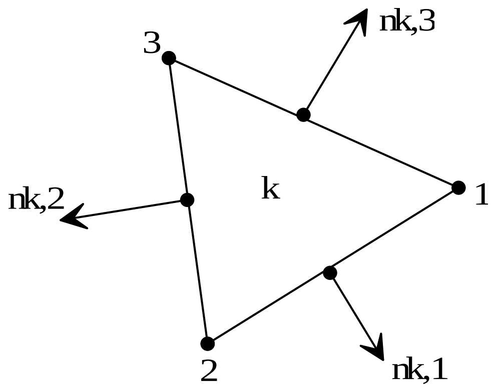

Figure 1. Volume element "*k*"

The four conserved variables of the solution vector Q_k are stored at the volume element *k*. Using Gauss' theorern in two dimensions, it as applied transforms surface integrals into line integrals, then Eq. (1) can be rewritten as:

$$\frac{d}{dt}\int_{\Omega} Q dA + \int_{\partial\Omega} \vec{F}.n ds = 0 \tag{5}$$

Where $\partial\Omega$ is the contour enclosing surface Ω and *n* is a vector outwardly normal to the surface. For volume *k*, this equation is discretized as**:**

$$\frac{dQ_k}{dt} = -\frac{1}{\Omega_k}\sum_{j=1}^{n_e} \vec{F}_{kj}.n_{kj} ds_{kj} = -\frac{1}{\Omega_k} R(Q_k) \tag{6}$$

Where *kj* represents the nodes index of triangle to left of edge *j* and to right of edge *j*. n_e is the total number of edges. The vector n_{kj} is the unit outward normal, ds_{kj} is the length of the edge *kj*, and $\vec{F}_{kj}$ is the numerical flux vector. The evaluation of the numerical flux in Eq. (6) is based on the Riemann problem defined by the solutions on the left and right of the volume edges, as in the first order MUSCL scheme given by (Van Leer, 1977). An important matrix of the 1D upwind schemes for systems of equations is the definition of the approximated flux Jacobian matrix *A* (Roe, 1986), built at the edges of the volume *k*. The 2D numerical upwind flux in Eq. (6) is obtained by applying the expression

$$\vec{F}_{ij} = \frac{1}{2}\left[\vec{F}_i + \vec{F}_j - \left|A_{ij}\right|(Q_j - Q_i)\right] \tag{7}$$

in a 1D form to each edge of the computational volume.
The numerical flux is finally written as

$$\vec{F}_{ij} = \frac{1}{2}[(\vec{F}_i + \vec{F}_j)_e.n_{ij} - \left[A_{ij}\right]_e (Q_j - Q_i)_e] \tag{8}$$

The *ij* used here represents the nodes index of triangle to left of edge and to right of edge as one goes from node 1 to node 2.

3. TIME INTEGRATION

The semi-discrete system given by eq. (6) can be integrated in time using explicit third order Runge-Kutta scheme (Cockburn and Shu, 1998) written as:

$$
\begin{aligned}
Q_k^{(1)} &= Q_k^{(n)} - \frac{\Delta t}{\Omega_k} R(Q_k^{(n)}) \\
Q_k^{(2)} &= \frac{3}{4} Q_k^n + \frac{1}{4}\left[Q_k^{(1)} - \frac{\Delta t}{\Omega_k} R(Q_k^{(1)}) \right] \\
Q_k^{n+1} &= \frac{1}{3} Q_k^n + \frac{2}{3}\left[Q_k^{(2)} - \frac{\Delta t}{\Omega_k} R(Q_k^{(2)}) \right]
\end{aligned}
\tag{9}
$$

The scheme as defined above is linearly stable for a CFL (Courant number) less than or equal 1.0 which is quite restrictive CFL condition. Convergence is accelerated using a local time stepping for steady state solutions. The local time step Δt on each volume Ω_k is determined by the following expression

$$
\frac{\Delta t}{\Omega_k} = \frac{CFL}{\sum_{e=1}^{3} C_{\max_e} d_e}
\tag{10}
$$

Where $C_{\max_e}$ is the maximum edge sound propagation speed, and d_e is the length of the edge. An illustration of a pseudo code is presented showing the edge data structure implemented in the solver.

```
do while (n < nstep)
      ! First step of RK3
      ! Calculate the flux at each interior edge
  do i = 1,Nedege
    flux calculation F
    residual calculation R
    edge sound velocity Cmax
    time step dt
enddo
! Apply bc at flux on each boundary edge
  do i = 1,Nbedge
     ! Outer boundary
     flux calculation F
     !Body boundary
     flux calculation F
     residual calculation R
     time step dt
  enddo
     !Local time step calculation dt/A
        dtA = CFL/dt
         Calculation of Q(1)
       ! Second step of RK3
       !...repeat as before
        Calculation of Q(2)
       ! Third step of RK3
       !...repeat as before
        Calculation of Q(n+1)
end do ! End iterative while
```

The time step is frozen at the first step of RK3.

3.1 Boundary Conditions

The cornputational domain presents two types of boundaries: the body boundary of the solid airfoil in the domain, and the far field boundary or outer-boundary. It need impose certain conditions in order to properly model the flow field. At body surface boundaries the normal component of the flow velocity is zero, then

$$\vec{F}.n = \{0; n_x p; n_y p; 0\} \tag{11}$$

where n is the local unit vector normal to the body surface and the pressure p is corrected by the tangential condition $V.n=0$. At the outer-boundary simple enforcement of freestream condition is applied.

4. NUMERICAL RESULTS

The following results are presented in an attempt to show that in some cases the solver here developed produces quite good results as it is assessed with experimental tests. The second order upwind scheme was robust enough to capture the first shock on the upper surface and also the secondary shock on the lower surface for the NACA0012. The subject of geometrical effects of the grid in this type of scheme plays an important role in obtaining a good numerical solution as will be shown in the following cases. All solutions presented in this section are initiated using a freestream start. The NACA0012 aerofoil at a freestream Mach number of 0.80 and angle of attack equal to 1.25 degrees in a transonic regime is simulated and appears to be a very difficult case as discussed by (Rizzi and Vivand, 1981). Rizzi and Vivand pointed out that in a number of numerical results given in (Rizzi and Vivand, 1981) all results obtained by potential solutions, except one, give no shock on the lower surface, whereas all the Euler solutions give one. This simulation is important to test the edge-based finite volume upwind scheme in order to capture the weak shock on the lower surface. The CFL of 0.9 is used. Figure 2 shows the residual history.

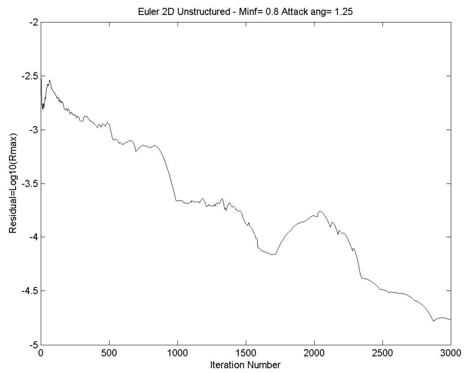

Figure 2. Residual history

In figure 3 the pressure coefficient is shown, and on the lower surface the Cp curve distribution shows the weak shock which can be easily identified. This Cp results are compared with the numerical results of case 9 in (AGARD, 1985) report. As can be seen the lower surface result show a good agreement, however the upper surface does not follow the (AGARD, 1985) result. Similar behavior is also shown in the (AGARD, 1985) for other numerical calculations using structured mesh with different grid sizes which does not invalidate the present result but justify how difficult is this test case.

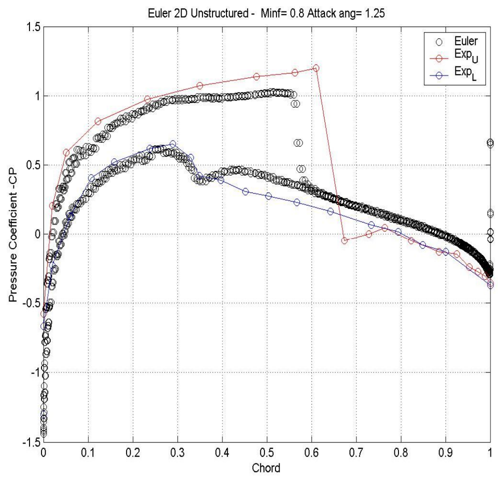

Figure 3. Cp comparison

In figure 4 the isobar lines are shown with interpolation lines number equal 30.

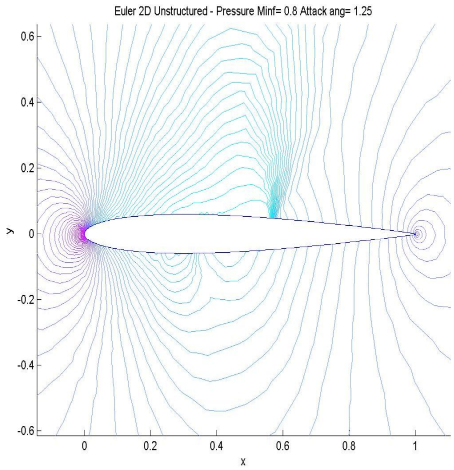

Figure 4. Isobar lines

The mesh used for this simulation has the following parameters: Number of Edge elements = 552, Number of elements = 10424, Number of unique vertices = 5488. The elapsed time taken was 8.451344e+003 seconds for the 3000 time steps. In figure 5 is depicted a close up of this mesh for illustration.

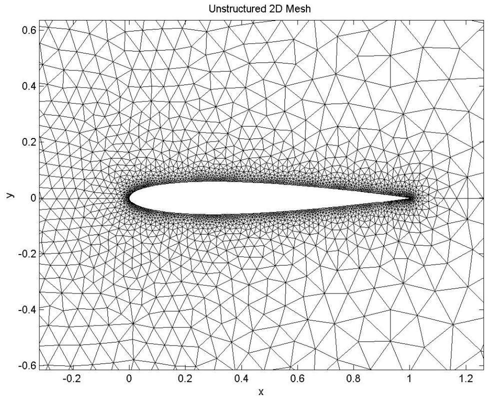

Figure 5. Unstructured mesh

The following results are for the cylinder case at Mach number of 2.0. In figure 6 is shown the color Mach flow field.

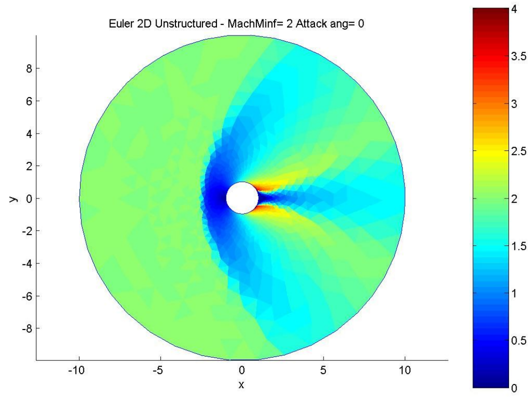

Figure 6. Isomach lines

It is shown in figure 7 the pressure contour.

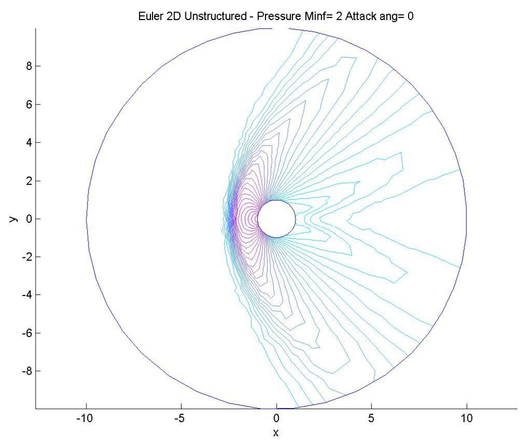

Figure 7. Isobar lines

The pressure distribution on the cylinder is shown in figure 8. It should be noted that the stagnation point pressure for a blunt body at zero degree of attack angle is analytically predicted by

$$\frac{p_0}{p_\infty} = \left(\frac{\gamma+1}{2} M_\infty^2\right)^{\frac{\gamma}{\gamma-1}} \cdot \left(1+\frac{2\gamma}{\gamma+1}(M_\infty^2-1)\right)^{-\frac{1}{\gamma-1}} \tag{12}$$

which is derived using the analogy of the Rayleigh formula for the supersonic Pitot tube and gives 5.64 while the numerically calculated value in this flow simulation is 5.81 indicating an error of less than 2.9%.

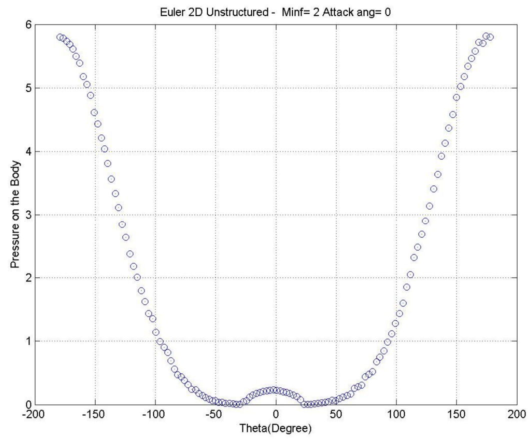

Figure 9. Pressure distribution the cylinder

The mesh used for this case is depicted in figure 9.

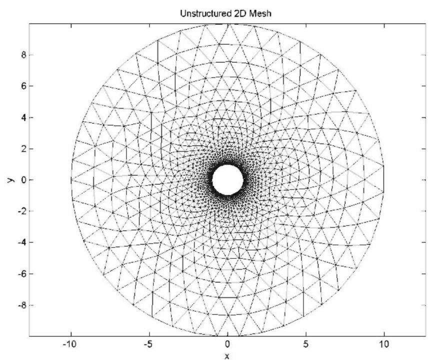

Figure 9. Unstructured Mesh

The following figures show a typical 2D blunt nosed cone vehicle configuration in supersonic Mach number of 2.0. The nose's radius is 0.8. In figure 10 is shown the Mach number flow field. The flow around a two-dimensional blunt nosed cone geometry in supersonic regime yields to a strong detached bow shock. It is also important to notice the symmetry of the flow field which is kept in the lower and upper regions of the domain.

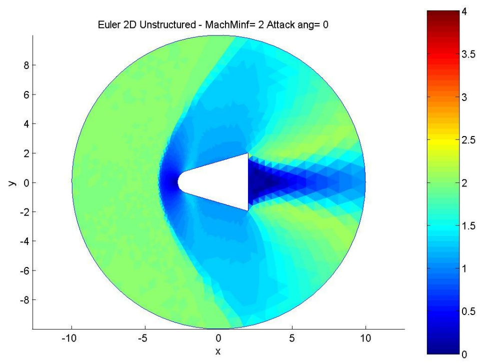

Figure 10. Mach flow field

The case for Mach 3.0 and attach angle of 15.0 degrees as shown as follow. Figure 11 show the Mach flow field.

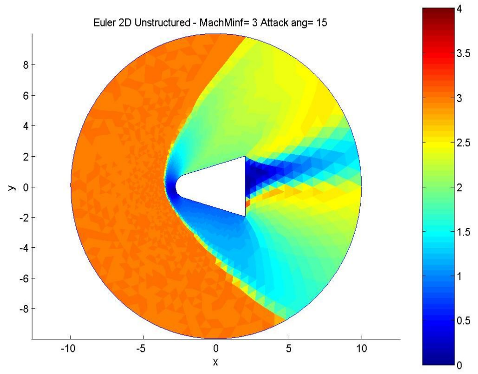

Figure 11. Mach flow field

5. CONCLUSION

The results presented for this benchmark case provide significant information that the edge-based finite volume upwind scheme can simulate the correct flow field with results comparable to results found in GAMM as in (Rizzi and Vivand, 1981) and AGARD as in (AGARD, 1985).

6. ACKNOWLEDGEMENTS

The author is very thankful for the kind help and attention given by Prof. Persson of MIT related to his *distmesh2d* mesh generator. This work has been fully supported by UFF at Volta Redonda campus.

7. REFERENCES

Barth, T.J., 1992. “Aspects of unstructured grids and finite-volume solvers for the Euler and Navier–Stokes equations”, Special Course on Unstructured Methods for Advection Dominated Flows, AGARD Report 787, pp. 6.1–6.61.
Barth, T.J., Ohlberger, M. 2004. “Finite volume methods: foundation and analysis”. Encyclopedia of Computational Mechanics. Edited by Erwin Stein, René de Borst and Thomas J.R. Hughes. John Wiley & Sons, Ltd.
Berglind, T. 2000. “An Agglomeration Algorithm for Navier-Stokes Grids”, AIAA-2000-2254.
Lyra, P.R.M., Lima, R.C.F., Guimarães, C.S.C. and De Carvalho, D.K.E., 2002. “An Edge-Based Unstructured Finite Volume Method for the Solution of Potential Problems, MECOM'2002 - First South American Congress on Computational Mechanics, Parana and Santa Fé, Argentina, pp. 1-19, published in CD-ROM.
Lyra, P.R.M., Lima, R.C.F., Guimarães, C.S.C. and De Carvalho, D.K.E. 2004. “An Edge-Based Unstructured Finite Volume”. Procedure for the Numerical Analysis of Heat Conduction Applications. J. of the Braz. Soc. of Mech. Sci. & Eng. Copyright. ABCM April-June, Vol. XXVI, No. 2, pp. 160-169.
Persson, P.O. and Strang, G., 2004. “A Simple Mesh Generator in MATLAB, *SIAM Review* 45, No2, 329-345.
Leer, B. van. 1977. “Towards the ultimate conservative difference scheme. IV. A new approach to numerical convection”. *Journal of Computational Physics*, 23(3):276–299.
Roe, P L., 1986. “Characteristic-based schemes for the Euler equations”. *Ann. Rev. Fluid Mech*., **18**, p337.
Cockburn, B. and C. W. Shu, 1998. “The Runge-Kutta Discontinuous Galerkin Method for conservation laws V: Multidimensional System”. Journal of Computational Physics, Vol. 141, pp. 199-224.
Rizzi, A. and Vivand, H., 1981. “Numerical Methods for the Computation of Inviscid Transonic Flows with Shock Waves”. Notes on Numerical Fluid Mechanics, Vol. 3, A GAMM Workshop, Vieweg and Sohn.
AGARD, 1985. “Test Cases for Inviscid Flow Methods”. AGARD Advisory Report n. 211, Essex, U.K.

8. RESPONSIBILITY NOTICE

The author is the only responsible for the printed material included in this paper.